Food and Chemical Toxicology 55 (2013) 386–395

Contents lists available at SciVerse ScienceDirect

Food and Chemical Toxicology

journal homepage: www.elsevier.com/locate/foodchemtox

Induction of HO-1 through p38 MAPK/Nrf2 signaling pathway by ethanol extract of *Inula helenium* L. reduces inflammation in LPS-activated RAW 264.7 cells and CLP-induced septic mice

Eun Jung Park [a], Young Min Kim [a], Sang Won Park [a], Hye Jung Kim [a], Jae Heun Lee [a], Dong-Ung Lee [b,*], Ki Churl Chang [a,*]

[a] Department of Pharmacology, School of Medicine, Institute of Health Sciences, Gyeongsang National University, Jinju 660-290, Republic of Korea
[b] Division of Bioscience, Dongguk University, Gyeongju 780-714, Republic of Korea

ARTICLE INFO

Article history:
Received 1 September 2012
Accepted 19 December 2012
Available online 5 January 2013

Keywords:
HMGB1
HO-1
Inflammation
Multiple organ failure
p38 MAPK
Mice

ABSTRACT

High mobility group box 1 (HMGB1) plays a crucial mediator in the pathogenesis of many inflammatory diseases. We recently proposed that heme oxygenase-1 (HO-1) negatively regulates HMGB1 in inflammatory conditions. We investigated whether ethanol extract of *Inula helenium* L. (EIH) activates p38 MAPK/Nrf2/HO-1 pathways in RAW264.7 cells and reduces inflammation in CLP-induced septic mice. EIH induced expression of HO-1 protein in a time- and concentration-dependent manner. EIH significantly diminished HO-1 expression in siNrf2 RNA-transfected cells. As expected, the inhibited expression of iNOS/NO, COX-2/PGE2, HMGB1 release by EIH in LPS-activated RAW264.7 cells was significantly reversed by siHO-1RNA transfection. Furthermore, EIH not only inhibited NF-κB luciferase activity, phosphorylation of IκBα in LPS-activated cells but also significantly suppressed expression of adhesion molecules (ICAM-1 and VCAM-1) in TNF-α activated human umbilical vein endothelial cells. The induction of HO-1 by EIH was inhibited by SB203580 but not by SP600125, PD98059, nor LY294002. Most importantly, administration of EIH significantly reduced not only increase in blood HMGB1, ALT, AST, BUN, creatinine levels but also decrease macrophage infiltrate in the liver of septic mice, which were reversed by ZnPPIX, a HO-1 inhibitor. We concluded that EIH has anti-inflammatory effect via the induction of p38 MAPK-dependent HO-1 signaling pathway.

1. Introduction

It has been shown that heme oxygenase-1 (HO-1) and its by-products play important roles in the resolution of inflammation (Otterbein et al., 1999; Ryter and Choi, 2006). High mobility group box-1 (HMGB1), a non-histone DNA-binding molecule, has been implicated as a multifunctional ubiquitous protein in many eukaryotic cells. HMGB1 was firstly found to be expressed in the nucleus, which regulates the cell cycle, cellular differentiation, and gene transcription (Bustin, 1999). In addition to its nuclear role, the pro-inflammatory cytokine-stimulating activity of extracellular HMGB1 has been proposed to be a crucial mediator in the pathogenesis of many diseases, including sepsis, arthritis, cancer, autoimmunity diseases, and diabetes (Lotze and Tracey, 2005; Andersson and Erlandsson, 2004; Ardoin and Pisetsky, 2008; Zhang et al., 2009). Moreover, HMGB1 is expressed in atherosclerotic lesions in humans and animals (Kalinina et al., 2004). Recently, we and others reported that HO-1 activity negatively regulates HMGB1 under systemic inflammatory conditions, such as sepsis (Jang et al., 2012; Tsoyi et al., 2009, 2011a; Takamiya et al., 2009).

Although *Inula helenium* L. (Compositae) and its active components have been widely used as anti-inflammatory, anti-microbial, and anti-cancer agents (Qiu et al., 2011; Dorn et al., 2006; Seo et al., 2008; Konishi et al., 2002), no report has found that the anti-inflammatory effect of *I. helenium* is related with HO-1 activity. Therefore, the present study tested the hypothesis that ethanol extract of *I. helenium* (EIH) induces HO-1 expression, which is responsible for the reduction of both pro-inflammatory mediators and HMGB1 release in LPS-activated macrophages. Since HO-1 couples the activation of mitochondrial biogenesis to anti-inflammatory cytokine expression, it might significantly reduce inflammatory

Abbreviations: ALT, alanine aminotransferase; AST, aspartate aminotransferase; BUN, blood nitrogen urea; CLP, cecal ligation and puncture; COX-2, cyclooxygenase 2; EIH, ethanol extract of *Inula helenium* L.; HO-1, heme oxygenase-1; HMGB1, high mobility group box 1; iNOS, inducible nitric oxide sythase; LPS, lipopolysaccharide.

* Corresponding authors. Tel.: +82 55 772 8071; fax: +82 55 772 8079 (K.C. Chang), tel.: +82 54 770 2224; fax: +82 55 742 9833 (D.-U. Lee).

E-mail addresses: dulee@dongguk.ac.kr (D.-U. Lee), kcchang@gnu.kr (K.C. Chang).

0278-6915/$ - see front matter © 2013 Elsevier Ltd. All rights reserved.
http://dx.doi.org/10.1016/j.fct.2012.12.027

cytokines. In addition, we explored the signal pathway(s) by which EIH up-regulates HO-1 induction. Here, we report that EIH inhibited expression of iNOS, COX-2, and HMGB1 release in LPS-activated macrophages as well as intercellular adhesion molecule 1 (ICAM-1) and vascular cell adhesion molecule 1 (VCAM-1) in TNF-α-activated human umbilical vein endothelial cells (HUVECs). Most importantly, administration of EIH significantly reduced the blood concentration of HMGB1 and attenuated multiple organ injury in cecal ligation and puncture (CLP)-induced mice, which were restored with zinc-protophorphyrin IX (ZnPPIX), a competitive inhibitor of HO-1, suggesting the importance of HO-1 induction by EIH for anti-inflammatory action.

2. Materials and methods

2.1. Materials

Dulbecco's modified Eagle's medium (DMEM), fatal bovine serum (FBS), and other tissue culture reagents were purchased from Gibco BRL Co. Primary antibodies for HO-1, cyclooxygenase-2 (COX-2), Nuclear factor erythroid 2 related factor 2 (Nrf2), PCNA, ICAM-1, VCAM-1, and responsible secondary antibodies used for Western blot analysis were purchased from Santa Cruz Biotechnology (Santa Cruz, CA). Antibodies for β-actin were from Sigma–Aldrich (St. Louis, MO), and inducible nitric oxide synthase (iNOS) were purchased from BD bioscience (San Jose, CA). Small interfering RNA for HO-1 (sc-44307) and Nrf2 (sc-37049) were purchased from Santa Cruz biotechnology (Santa Cruz, CA), and scrambled siRNA was purchased from Invitrogen (Carlsbad, CA). Enzyme-linked immunosorbent assay (ELISA) kit for prostaglandin E2 (PGE_2) and HMGB1 was purchased from Shino test Corp. (Tokyo, Japan). Alanine aminotransferase (ALT), aspartate aminotransferase (AST), and blood urea nitrogen (BUN) assay kits were obtained from IVD Lab Corp. (Uiwang, Korea). Enzymatic creatinine reagent kit was purchased from (Sekisui Medical, Tokyo, Japan).

2.2. Preparation of plant extract

Roots of *I. helenium* (cultivated in Jaechun, Chungbuk, Korea) were provided and authenticated by Professor Je-Hyun Lee (College of Oriental Medicine, Dongguk University, Korea). The dried roots (115 g) were ground to powder and extracted with 70% ethanol twice at 95 °C for 3 h. The combined extracts were filtered and concentrated under reduced pressure to give 40.6 g of crude extracts (yield 35.3%). The main fraction of crude extract is a non-polar hexane fraction, which was identified to contain some sesquiterpenoid compounds, including isoalantolactone (39% content), β-elemene, valencene, and germacrene A (all <1% contents) as analyzed by GC–MS (data not shown).

2.3. Cell culture

RAW264.7 macrophages were maintained at 5×10^5 cells/ml in DMEM supplemented with 10% heat-inactivated FBS, penicillin (100 units/ml), streptomycin (100 mg/ml), L-glutamine (4.5 mg/ml), and glucose (4.5 mg/ml), followed by incubation at 37 °C in a humidified atmosphere containing 5% CO_2 and 95% air. For analysis of ICAM-1 and VCAM-1 expression, EA hy926 cells, a human umbilical vein endothelial cell line, were cultured at a density of 1×10^7 cells/100 mm dish.

2.4. Western blot analysis

Western blot analysis was performed by lysing cells in RIPA buffer (25 mM Tris-HCl; pH 7.4, 150 mM NaCl, 1% NP-40, 1% sodium deoxycholate, 0.1% SDS) containing a protease inhibitor mixture. Protein concentration was determined using Bradford assay; absorbance of the mixture at 595 nm was determined using an ELISA plate reader. An equal amount of protein for each sample was resolved using 8–10% sodium dodecyl sulfate–polyacrylamide gel electrophoresis (SDS–PAGE), followed by electrophoretic transfer onto PVDF Western blotting membranes (Roche, Germany). The membrane was then blocked with 5% skim milk and sequentially incubated with primary antibody and horseradish peroxidase-conjugated secondary antibody, followed by ECL detection (Animal Genetics).

2.5. NOx measurement

The nitrite and nitrate (NOx) concentrations in the medium were measured as an indicator of NO production, according to Kang et al. (1999). Each supernatant (100 μl) was mixed with the same volume of Griess reagent; absorbance of the mixture at 545 nm was determined with an ELISA plate reader.

2.6. PGE_2 measurement

RAW264.7 macrophages were seeded in a 60-mm cell culture dish, pre-incubated for 1 h with different concentrations of EIH, and then stimulated for 16 h with LPS. Supernatant of the culture medium (100 μl) was then collected for the determination of PGE_2 concentrations using the ELISA kit.

2.7. Cytokine assays

Concentrations of TNF-α or IL-1β in culture supernatants were determined using ELISA kits (R&D Systems) according to the instructions provided by the manufacturer. Concentrations of TNF-α or IL-1β were calculated with standard curves.

2.8. MTT

For determination of cell viability, 50 mg/ml of thiazolyl blue tetra-zolium bromide (MTT) was added to 1 ml of cell suspension (3×10^5 cells/ml in 24-well plates) for 4 h, and the formazan formed was dissolved in DMSO; optical density was measured at 570 nm.

2.9. siRNA and vector transfection

The RAW 264.7 macrophages were seeded into 60-mm cell culture dishes at 3×10^5 cells/dish 18–24 h prior to transfection. Cells were transfected with 2 μg of NF-κB luciferase vector, 100 nM si-Nrf2 RNA, 100 nM siHO-1 RNA, 100 nM scramble siRNA, or si-p38 MAPK RNA using SuperFect fragment (Qiagen, Valencia, CA). After 4 h of incubation, the medium was replaced with a fresh medium.

2.10. NF-kB luciferase activity

After the scheduled treatment, cells were washed twice with cold PBS, lysed in lysis buffer provided in the dual luciferase kit (Promega, Madison, WI), and assayed for luciferase activity using a TD-20/20 luminometer (Tumer Designs, Sunnyvale, CA), according to the manufacturer's protocol. All transfections were done in triplicate. Data are presented as the ratio between Firefly and renilla luciferase activities.

2.11. HO-1 activity

The harvested cells were subjected to three cycles of freeze–thawing before addition to a reaction mixture consisting of phosphate buffer (1 ml final volume, pH 7.4) containing magnesium chloride (2 mM), NADPH (0.8 mM), glucose-6-phosphate (2 mM), glucose-6-phosphate dehydrogenase (0.2 units), rat liver cytosol as a source of biliverdin reductase, and the substrate hemin (20 μM). The reaction mixture was incubated in the dark at 37 °C for 1 h and was terminated by the addition of 1 ml of chloroform. After being vigorously vortexed and centrifuged, the extracted bilirubin in the chloroform layer was measured by the difference in absorbance between 464 and 530 nm ($\varepsilon = 40\ mM^{-1}\ cm^{-1}$).

2.12. Animal study

The CLP-induced sepsis model was implemented as described previously (Tsoyi et al., 2009). In brief, BALB/c mice (male, 7–8 weeks old, 20–25 g) were anesthetized with ketamine (30 mg/kg) and xylazine (6 mg/kg). Next, a 2-cm midline incision was made to allow exposure of the cecum and adjoining intestine. The cecum was tightly ligated with a 3.0-silk suture at its base below the ileo-cecal valve, and was punctured twice (top and bottom) through both cecal walls with an 18-gauge needle. The cecum was then gently squeezed to extrude a small amount of feces from the perforation sites and returned to the peritoneal cavity. The laparotomy site was then stitched with 4.0 silk. In Sham-control animals, the cecum was exposed but not ligated or punctured and then returned to the abdominal cavity. Mice were maintained in accordance with the Guide for the Care and Use of Laboratory Animals (NIH publication 85-23, revised 1996). The protocol was approved in advance by the Animal Research Committee of Gyeongsang National University. Mice were divided into five groups: Sham ($n = 3$), CLP ($n = 5$), EIH + CLP (i.p., 5 mg/kg, $n = 5$), EIH + CLP (i.p., 10 mg/kg, $n = 6$), and ZnPPIX (i.p., 10 mg/kg, $n = 5$) + EIH (i.p., 10 mg/kg)+CLP. EIH or ZnPPIX was injected (i.p) 2 h prior to surgery. All animals received subcutaneous administration of 1 ml of normal saline immediately after the operation for fluid resuscitation.

2.13. Blood HMGB1 level and multiple organ damage parameters in CLP-induced septic mice

Twenty-four hours after completion of the CLP operation, blood was withdrawn by cardiac puncture from animals in each group anesthetized with ketamine (30 mg/kg) and xylazine (6 mg/kg). Plasma ALT and AST activities were determined in the collected blood samples by employing standard spectrophotometric procedures using ChemiLab ALT and AST assay kits (IVD Lab Co., Ltd., Uiwang, Korea). The BUN level was measured using a ChemiLab BUN assay kit (IVD Lab Co., Ltd.,

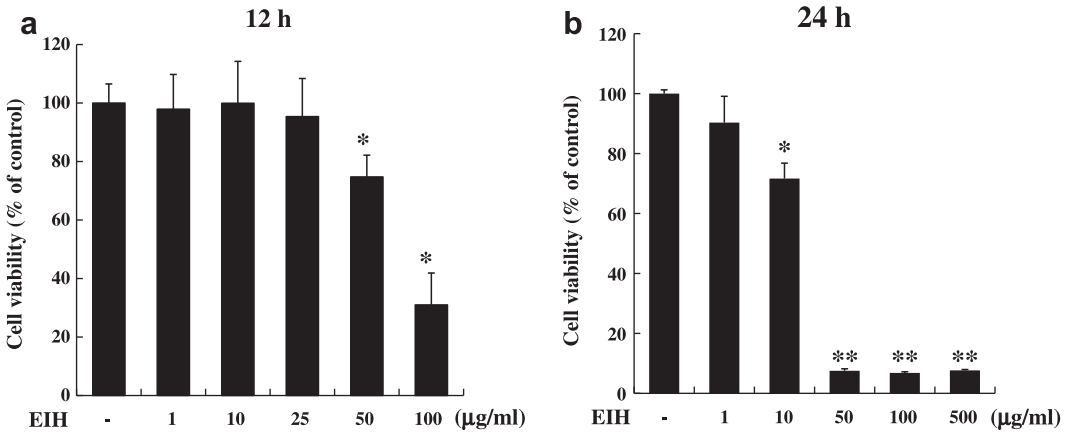

Fig. 1. Cytotoxic effect of EIH in RAW 264.7 cells. Cell viability was determined by MTT. Cells were treated with different concentrations of EIH for 12 h (a) and 24 h (b). The results are expressed as the means ± SE of three independent experiments. $^{*}p < 0.05$, $^{**}p < 0.01$ compared to control, respectively.

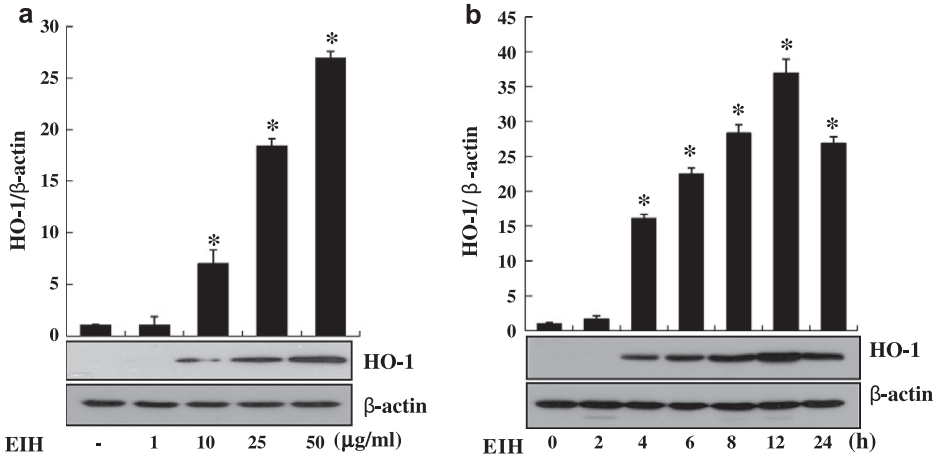

Fig. 2. Effect of EIH on HO-1 expression. Expression of HO-1 by EIH was examined in a concentration-dependent manner with different doses after 8 h of treatment (a) and in a time-dependent manner with 25 μg/ml of EIH (b). After completion, proteins were extracted and Western blot analysis performed using anti-HO-1 antibody. The results are expressed as the means ± SE of three independent experiments. $^{*}p < 0.05$ compared with control.

Uiwang, Korea) according to the manufacturer's instructions. Plasma creatinine was measured using an enzymatic creatinine reagent kit (Sekisui Medical, Tokyo, Japan). This method of creatinine measurement largely eliminates interference from mouse plasma chromagens well known to the Jaffe method (Slot, 1965). HMGB1 (Shino-Test Corp., Tokyo, Japan) was determined using an ELISA kit according to the manufacturer's instructions.

2.14. Immunohistochemistry

The depafaffinized section from liver was placed in a solution of 1% H_2O_2 for 10 min. After washing, the section was treated with 5% blocking serum for 1 h at room temperature. The slide was incubated overnight at 4 °C in a humidified chamber with anti-rabbit-F4/80 (1:50; Santa Cruz Biotechnology). After washing three times with 0.1 M PBS, the section was incubated for 1 h at room temperature with secondary biotinylated antibody (1:100). After washing, the section was incubated in avidin–biotin-peroxidase complex solution (Vector Laboratories, Burlingame, CA). The section was developed with 0.05% diaminobenzidine (Sigma–Aldrich) containing 0.05% H_2O_2, dehydrated, and coverslipped with Permount (Sigma–Aldrich). The section was visualized by CKX41 light microscopy (Olympus).

2.15. Statistical evaluation

Scanning densitometry was performed using an Image Master® VDS (Pharmacia Biotech Inc., San Francisco, CA). Data are expressed as the mean ± SE of results obtained from the number of replicate treatments. Differences between data sets were assessed by one-way analysis of variance followed by Newman-Keuls tests. $p < 0.05$ was accepted as statistically significant.

3. Results

3.1. Effect of EIH on cell viability

Cells were treated with different concentrations of EIH, and MTT assay was performed after 12 h of incubation as described in Section 2. As shown in Fig. 1a, an approximately 80% survival rate was observed at a dose of 50 μg/ml. However, when incubated for 24 h, significant toxic signs were observed at above 50 μg/ml of EIH (Fig. 1b). Therefore, through the entire experiments, the maximum concentration of EIH was limited to 50 μg/ml.

3.2. EIH increases HO-1 expression

Fig. 2 shows that EIH significantly increased HO-1 protein expression in a time- and concentration-dependent manner in RAW 264.7 cells. At a fixed concentration of EIH (25 μg/ml), HO-1 was expressed as early as 4 h and continuously increased until 12 h, after which it diminished until 24 h (Fig. 2b).

3.3. EIH inhibits expression of pro-inflammatory genes and related mediators

Fig. 3a shows that EIH dose-dependently inhibited expression of iNOS protein as well as NOx production in LPS-stimulated RAW

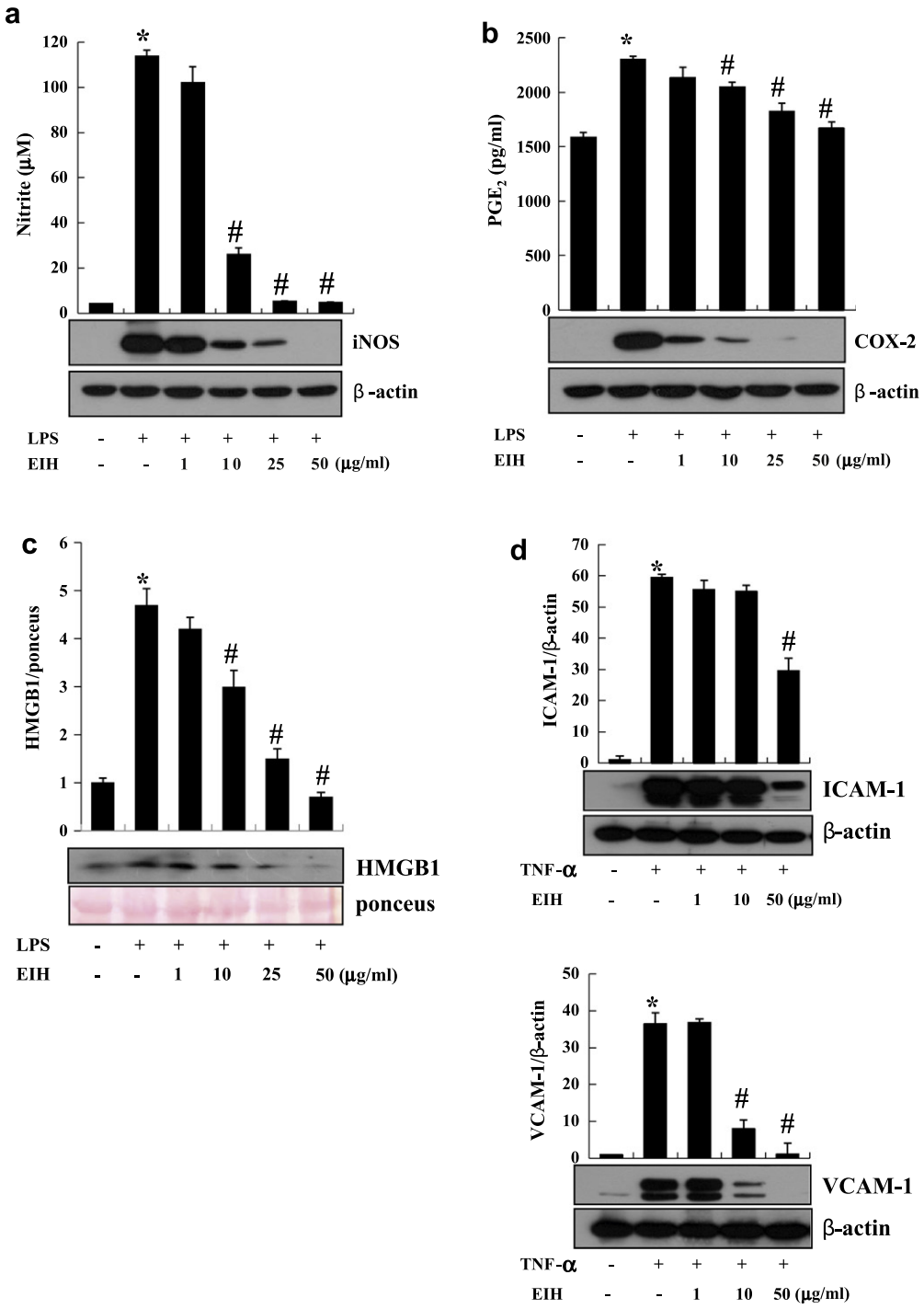

Fig. 3. Anti-inflammatory effect of EIH. RAW 264.7 cells were stimulated with different concentrations of EIH for 1 h prior to LPS (1 μg/ml) treatment, followed by incubation for 8 h for detection of iNOS and COX-2 or 16 h for HMGB1. Endothelial cells stimulated with different concentrations of EIH for 1 h prior to TNF-α (10 ng/ml) treatment, followed by incubation for 8 h for detection of ICAM-1 and VCAM-1. Proteins were extracted and subjected to Western blot analysis for iNOS (a), COX-2 (b), HMGB1 (c), and adhesion molecules (ICAM-1 and VCAM-1). Production of NO (a), PGE_2 (b), TNF-α and IL-1β (e) from the culture medium was measured as described in Section 2. Since HMGB1 was released into the media from the cells, we used ponceus as a loading control. The results are expressed as the means ± SE of three independent experiments. $^{*}p < 0.05$ compared with untreated cells. $^{\#}p < 0.05$ compared with LPS-treated cells or TNF-α-activated endothelial cells, respectively.

264.7 cells. As a control, LPS, which is bacterial endotoxin, significantly up-regulated iNOS protein and subsequently increased NO production. However, in the presence of EIH, up-regulation of iNOS induced by LPS was significantly inhibited. For example, 10 μg/ml of EIH decreased NO production to a level 80% that of the LPS control. COX-2 enzyme is also an important mediator of inflammation. As expected, EIH significantly and dose-dependently decreased the expression of COX-2 as well as PGE_2 production (Fig. 3b). Interestingly, the concentration of EIH that reduced iNOS and COX-2 protein expression was sufficient to inhibit LPS-induced HMGB1 release (Fig. 3c) and protein expression of ICAM-1 and VCAM-1 in TNF-α-stimulated endothelial cells (Fig. 3d). This result was in

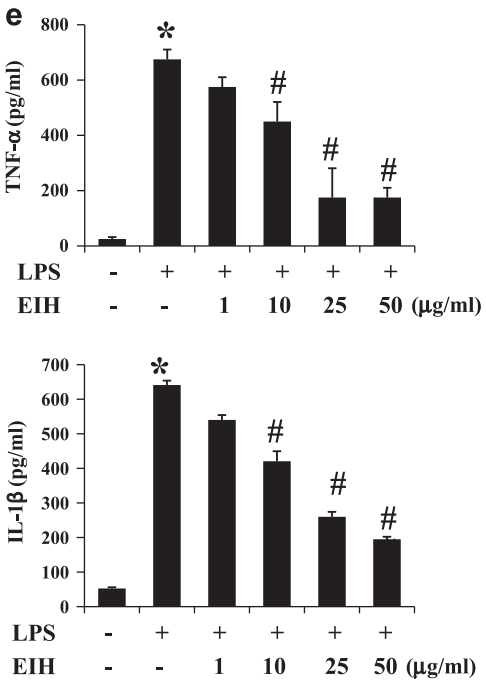

Fig. 3. (*continued*)

good agreement with the EIH concentration that could induce HO-1 protein expression. In addition, EIH significantly reduced LPS-activated TNF-α and IL-1β levels in RAW 264.7 cells (Fig. 3e).

3.4. EIH induces HO-1 expression by Nrf2 translocation

Nrf2 plays an important role in the induction of HO-1 in many cells, including macrophages. Therefore, we determined whether or not EIH-mediated HO-1 induction is related to activation of Nrf2. As shown in Fig. 4a, Nrf2 was retained in the cytosolic fraction in untreated cells, whereas it was translocated to the nuclear fraction at a higher concentration of EIH. To further confirm that EIH could activate Nrf2 translocation, we used small interfering RNA (siRNA). Increased HO-1 protein expression by EIH was significantly diminished in Nrf2 siRNA-transfected cells, whereas scrambled siRNA-transfected cells displayed similar HO-1 expression as EIH-treated cells (Fig. 4b). As expected, EIH increased HO-1 activity in a concentration-dependent manner (Fig. 4c).

3.5. EIH inhibits NF-κB activity

NF-kB is a well known transcription factor leading to the induction of pro-inflammatory genes, such as iNOS, COX-2, ICAM-1, and VCAM-1. Thus, we measured NF-κB luciferase activity to determine whether or not EIH inhibits NF-κB activation. Fig. 5a clearly shows that EIH dose-dependently inhibited LPS-induced NF-κB luciferase activity. To further confirm this result, we measured IκBα phosphorylation and translocation of NF-κB. As expected, EIH dose-dependently mediated the translocation NF-κB from the cytosolic (CE) to nuclear fraction (NE) and diminished the p-IκBα level (Fig. 5b and c).

3.6. HO-1 is crucial for anti-inflammatory effect of EIH

To determine whether or not HO-1 induction is critical for the anti-inflammatory action of EIH, we measured the expression of iNOS and COX-2 proteins in HO-1 siRNA-transfected cells after confirming the transfection efficacy of HO-1 siRNA (Fig. 6a). We found that the inhibition of iNOS/NO (Fig. 6b) and COX-2/PGE_2 (Fig. 6c) expression by EIH was reversed in HO-1 siRNA-transfected cells, indicating that HO-1 enzyme plays a key role in the anti-inflammatory action of EIH.

3.7. Signal mechanism responsible for induction of HO-1 by EIH

Finally, we determined the mechanism by which EIH induces HO-1 expression in macrophage cells. The p38 MAPK/Nrf2 signaling pathway has been reported to induce HO-1 expression (Jang et al., 2012). Fig. 7a shows that SB203580, a p38 MAPK inhibitor, strongly reduced the HO-1 protein expression induced by EIH. However, SP600125, PD98059, and LY294002 all had no effect on HO-1 protein expression. To elucidate whether or not p38 MAPK mediates the effect of EIH on HO-1 expression, phosphorylation of p38 MAPK was measured. Fig. 7b and c shows that EIH up-regulated p-p38 MAPK in a time- and concentration-dependent manner. The involvement of p38 MAPK in HO-1 induction by EIH was verified by testing iNOS expression in the presence of different MAPK inhibitors (Fig. 7d). It was found that only SB203580 reversed the inhibitory effect of EIH on LPS-induced iNOS expression, indicating the importance of p38 MAPK signaling for the action of EIH. To further confirm the involvement of p38 MAPK in induction of HO-1, we determined whether or not EIH reduces HO-1 expression in p38 siRNA-transfected cells. We found that EIH significantly reduced HO-1 expression in p38 siRNA-transfected cells but not control siRNA-transfected cells (Fig. 7e). In contrast, other MAPK inhibitors or PI3K inhibitor had no effect on the induction of iNOS by LPS. Signal inhibitors did not modify the effect of LPS by themselves.

3.8. HO-1-dependent protective effect of EIH in CLP-induced septic mice

As shown above, we investigated a possible linkage between HO-1 induction and the anti-inflammatory effect of EIH *in vitro*. To understand the anti-inflammatory action of EIH through HO-1, we used a CLP-induced septic mice model. As shown in Table 1, CLP-induced septic mice clearly displayed liver and kidney damage, as indicated by increases in plasma ALT, AST, BUN, and creatinine levels. However, treatment with EIH at two different doses (5 and 10 mg/kg) significantly reduced plasma ALT, AST, BUN, and creatinine levels in CLP-induced septic mice. Likewise, the blood HMGB1 level was significantly reduced by administration of EIH in CLP-induced mice. Importantly, the reduced blood levels of AST, BUN, and HMGB1 were reversed by ZnPP IX, an HO-1 inhibitor, indicating the importance of HO-1 to the anti-inflammatory action of EIH *in vivo* (Fig. 8a). Finally, to confirm whether or not the infiltrated inflammatory cells are reduced by EIH treatment in CLP-induced septic mice, liver tissues were stained using F4/80-corresponding antibody, a macrophage marker. It was clearly shown that EIH significantly reduced the infiltration of inflammatory cells into liver tissues of CLP-induced mice (Fig. 8b).

4. Discussion

This study, for the first time, provides evidence for the mechanism by which EIH mediates its anti-inflammatory responses by inducing HO-1 *in vitro* and *in vivo*. HO-1 and its by-products (biliverdin, CO) are known to have cyto-protective properties, including anti-oxidant, anti-inflammatory, and anti-apoptotic activities (Otterbein et al., 1999; Ryter and Choi, 2006). There is increasing evidence demonstrating that the induction of HO-1 can prevent or mitigate the symptoms associated with related ailments in experimental models of acute inflammation (Kobayashi et al.,

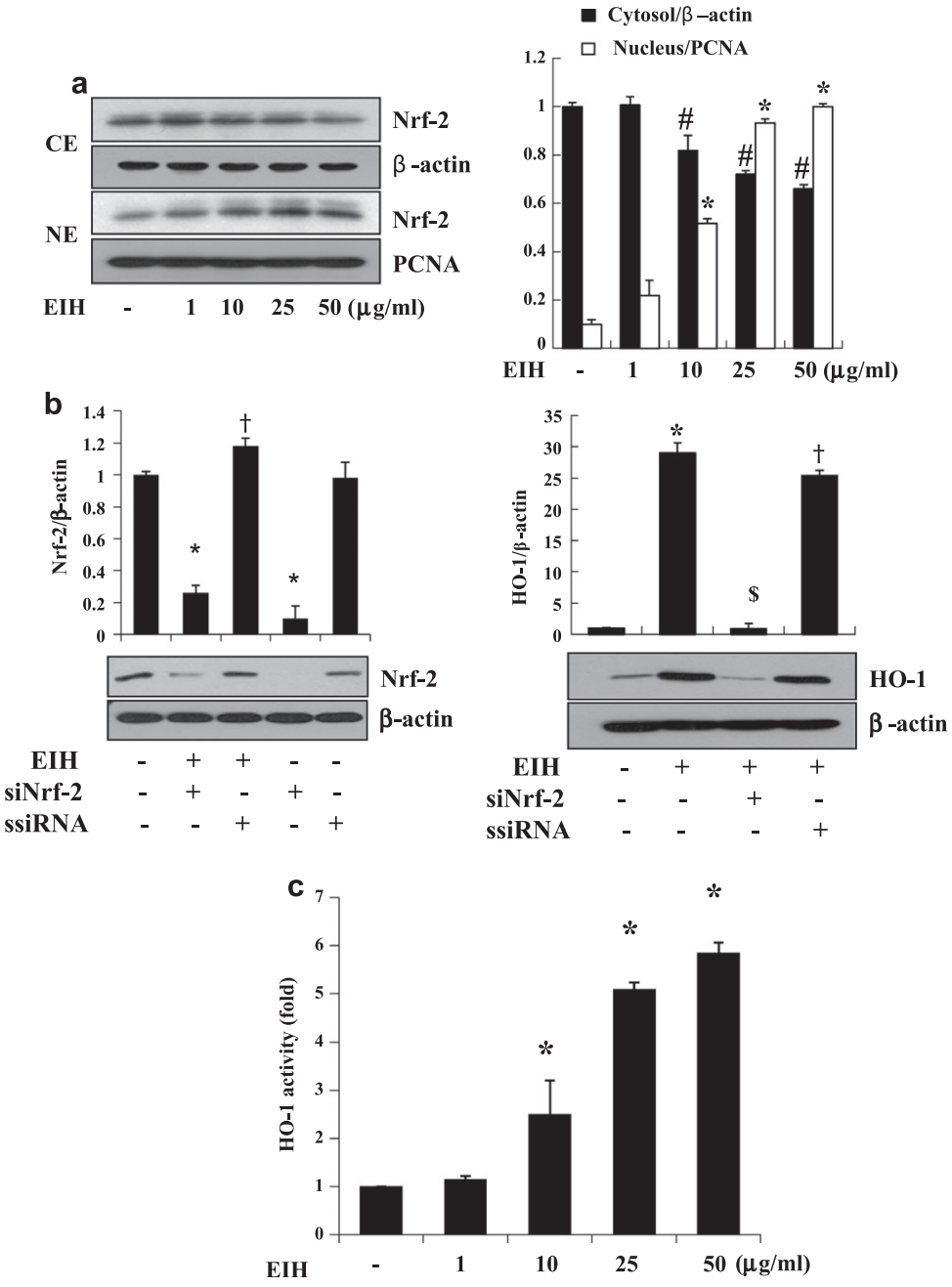

Fig. 4. Effect of EIH on Nrf2 translocation in macrophages. EIH was treated at different concentrations (0, 1, 10, 25, and 50 μg/ml) for 3 h. Cytosolic extracts (CE) and nuclear extracts (NE) were subjected to SDS–PAGE, and Nrf2 was detected by immunoblotting (a). To determine whether or not Nrf2 is involved in HO-1 induction by EIH, cells were transfected with either siNrf2 RNA or scrambled siRNA (ssiRNA), and transfection efficacy was confirmed by expression of Nrf2 with EIH (b). siNrf2 RNA- or ssiRNA-transfected cells were treated with EIH and incubated for 8 h, followed by Western blot analysis using anti-HO-1 antibody. HO-1 activity was measured (c). The results are expressed as the means ± SE of three independent experiments. $^{*,\ \#}p < 0.05$ compared with untreated cells, respectively. $^{\$}p < 0.05$ compared with EIH-treatment. $^{\dagger}p < 0.05$ compared with EIH+siNrf-2.

2006). Therefore, targeted over-expression of HO-1 may be beneficial for the treatment of inflammatory disorders. Many phytochemicals in plants are recognized as HO-1 inducers and are traditionally used in therapeutic strategies for chronic inflammatory diseases (Hwa et al., 2012; Tsoyi et al., 2011a; Jun et al., 2012; Joe et al., 2012). Increasing evidence indicates that induction of HO-1 is closely linked to Nrf2 activation (Kim et al., 2012; Shin et al., 2012; Jang et al., 2012). In addition, many kinase signaling pathways, including PKC, PI3K/Akt, ERK, JNK, and p38, may regulate Nrf2 activation and facilitate its accumulation in the nucleus for the promotion of HO-1 gene expression (Jang et al., 2012; Jun et al., 2012). The present results indicated that SB203580 (p38 MAPK inhibitor), but not SP600125 (JNK inhibitor), PD98059 (ERK inhibitor), or LY294002 (PI3K inhibitor), significantly inhibited HO-1 induction induced by EIH. Indeed, involvement of p38 MAPK is well documented in many diseases, including inflammatory disorders. Recently, our laboratory found evidence that ethyl pyruvate, a potent anti-inflammatory agent, induces HO-1 expression through a p38 MAPK/Nrf2-dependent pathway by decreasing glutathione cellular levels in RAW 264.7 cells (Jang et al., 2012). In contrast, activation of the p38/Nrf2 pathway causes down-regulation of HO-1 expression in RAW 264.7 cells (Naidu et al., 2009).

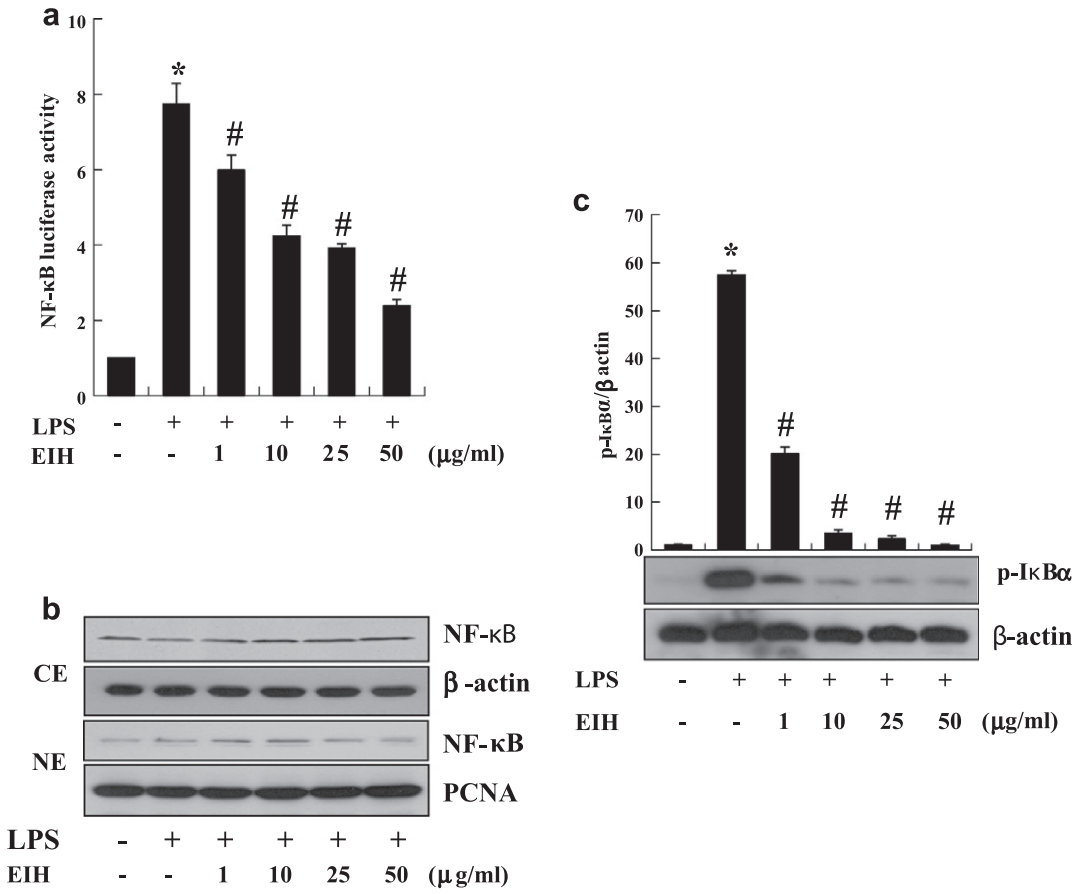

Fig. 5. Inhibition of NF-κB activation by EIH in RAW 264.7 cells. Cells were pretreated with EIH (1, 10, 25, and 50 μg/ml) for 1 h, followed by incubation for another 1 h with LPS (1 μg/ml). After treatment, NF-kB luciferase activity was measured in cells transiently transfected with NF-kB luciferase (a), NF-κB (b) and phosphor-IκBα (c) levels were determined by Western blot analysis. The results are expressed as the means ± SE of three independent experiments. $^{*}p < 0.05$ compared with untreated cells. $^{\#}p < 0.05$ compared with LPS-treated cells.

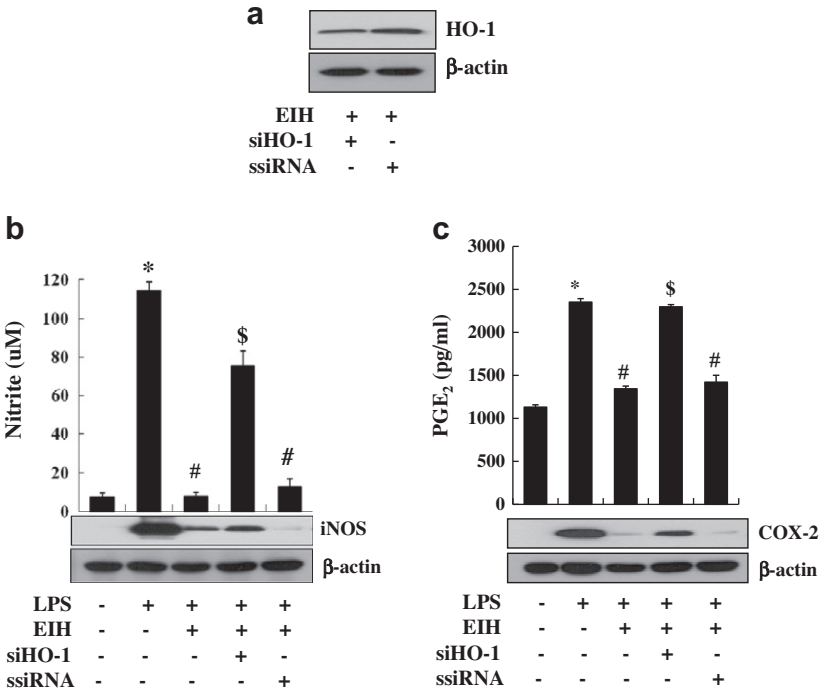

Fig. 6. Effects of EIH on expression of iNOS and COX-2 in HO-1 siRNA-transfected macrophages. Cells were transfected with either siHO-1 RNA or scrambled siRNA (ssiRNA), and transfection efficacy was confirmed by expression of HO-1 with EIH (a). siHO-1RNA- or ssiRNA-transfected cells were treated with EIH and incubated for 8 h, followed by Western blot analysis using anti-iNOS (b) or anti-COX-2 antibody (C), respectively. The results are expressed as the means ± SE of three independent experiments. $^{*}p < 0.05$ compared with untreated cells. $^{\#}p < 0.05$ compared with LPS-treatment. $^{\$}p < 0.05$ compared with EIH + LPS-treatment.

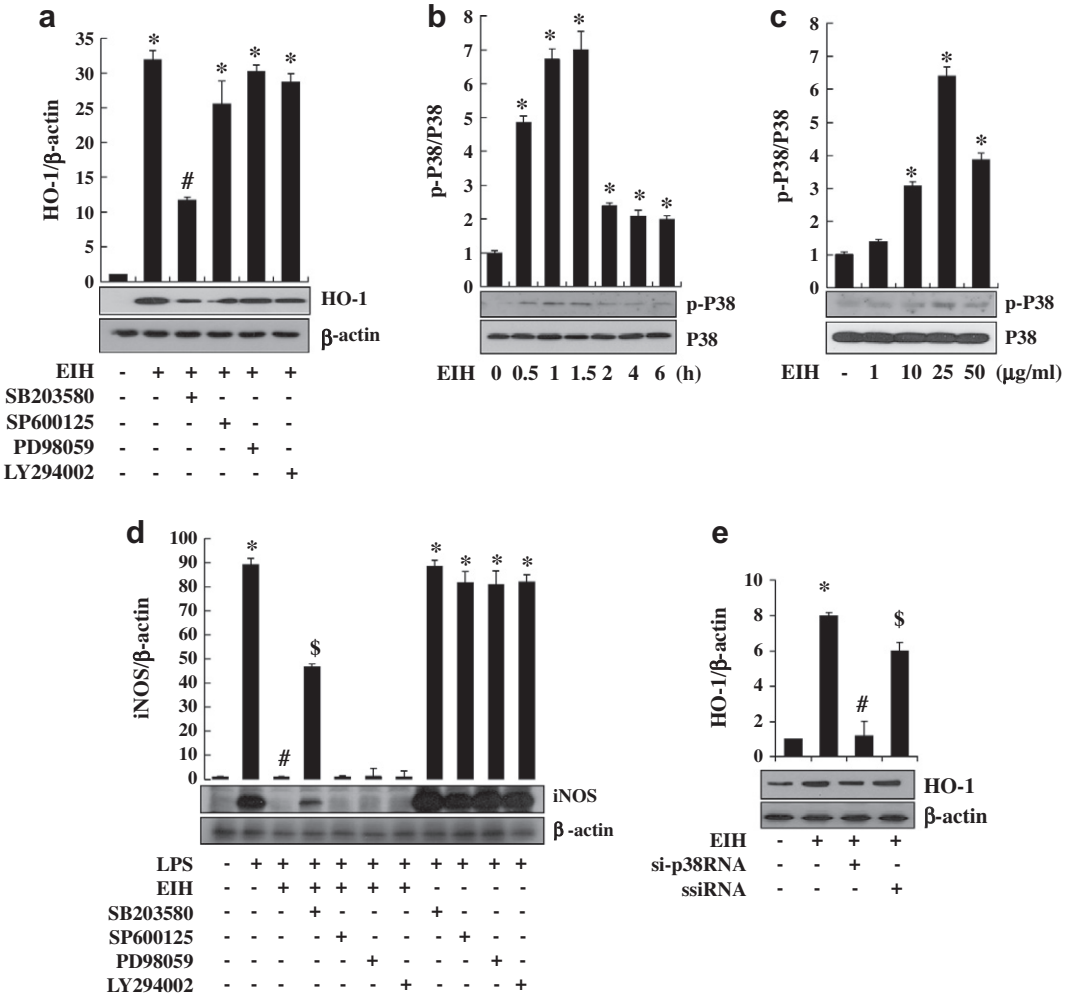

Fig. 7. Signal pathways of EIH in HO-1 expression. Cells were exposed to SB203580 (10 μM), SP600125 (40 μM), PD98059 (50 μM), or LY294002 (10 μM) for 1 h, followed by stimulation with EIH (25 μg/ml) for 8 h. Then, the HO-1 protein level was determined by Western blot analysis (a). Cells were treated with EIH (25 μg/ml) for different times as indicated (b) or for a fixed time (1 h) with different concentrations of EIH (c). To further confirm that the anti-inflammatory effect of EIH is mediated by p38 MAPK, inhibition of iNOS by EIH was tested in the presence of different signal inhibitors in LPS-activated cells (d). HO-1 expression by EIH was significantly diminished by p38 deletion but not control siRNA transfection (e). As a positive control, the effects of signal inhibitors on iNOS expression were investigated in the presence of LPS. The results are expressed as the means ± SE of three independent experiments. $^{*}p < 0.05$ compared with untreated cells. $^{\#}p < 0.05$ compared EIH- or LPS-treated cells. $^{\$}p < 0.05$ compared EIH + LPS- or si-p38 RNA-treated cells.

Table 1
HO-1-dependent protective effect of EIH in CLP-induced septic mice.

Treatment	ALT activity (U/L)	AST activity (U/L)	BUN (U/L)	Creatinine (mg/dL)
Sham	64.0 ± 11.2	392.3 ± 17.2	16.9 ± 2.9	0.9 ± 0.3
CLP	328.6 ± 68.6**	1130.5 ± 87.5**	65.5 ± 7.3**	2.1 ± 0.5**
CLP + EIH (5 mg/kg)	104.8 ± 34.5##	672.8 ± 16.5##	33.6 ± 9.4##	1.6 ± 0.4
CLP + EIH (10 mg/kg)	120.5 ± 27.1##	593.6 ± 138.3##	16.9 ± 10.7##	1.1 ± 0.3##
CLP + EIH (10 mg/kg)+ZnPP IX (10 mg/kg)	143.2 ± 34.5	915.5 ± 205.2$$	62.0 ± 5.6$$	1.4 ± 0.4

Mice were intraperitoneally administered with 5 mg/kg or 10 mg/kg EIH 2 h prior to CLP. Twenty-four hours after CLP, blood was withdrawn under anesthesia by heart puncture from each group of animals. The results are presented as mean ± SE ($n = 3–6$).
** $p < 0.05$ significantly different from sham.
$p < 0.01$ significantly different from CLP.
$$ $p < 0.01$ significantly different from CLP + EIH (10 mg/kg).

This observation indicates that p38 may have a dual function in HO-1 gene regulation. However, others have reported that p38 MAPK/Nrf2 is required to increase the expression of HO-1 by epigallocatechin, the major polyphenol in green tea, in vascular smooth muscle cells, suggesting that the p38 MAPK/Nrf2/HO-1 signaling pathway is not limited to macrophages (Pullikotil et al., 2011). In this regard, it is interesting to note that alantolactone, one of the active ingredients of EIH, induces phase 2 detoxifying enzymes in HepG2-C8 cells (Seo et al., 2008).

HO-1 induction has also been shown to inhibit the expression of pro-inflammatory mediators through inactivation of NF-κB (Ha et al., 2012). There are reports that p65 represses Nrf2 transcription

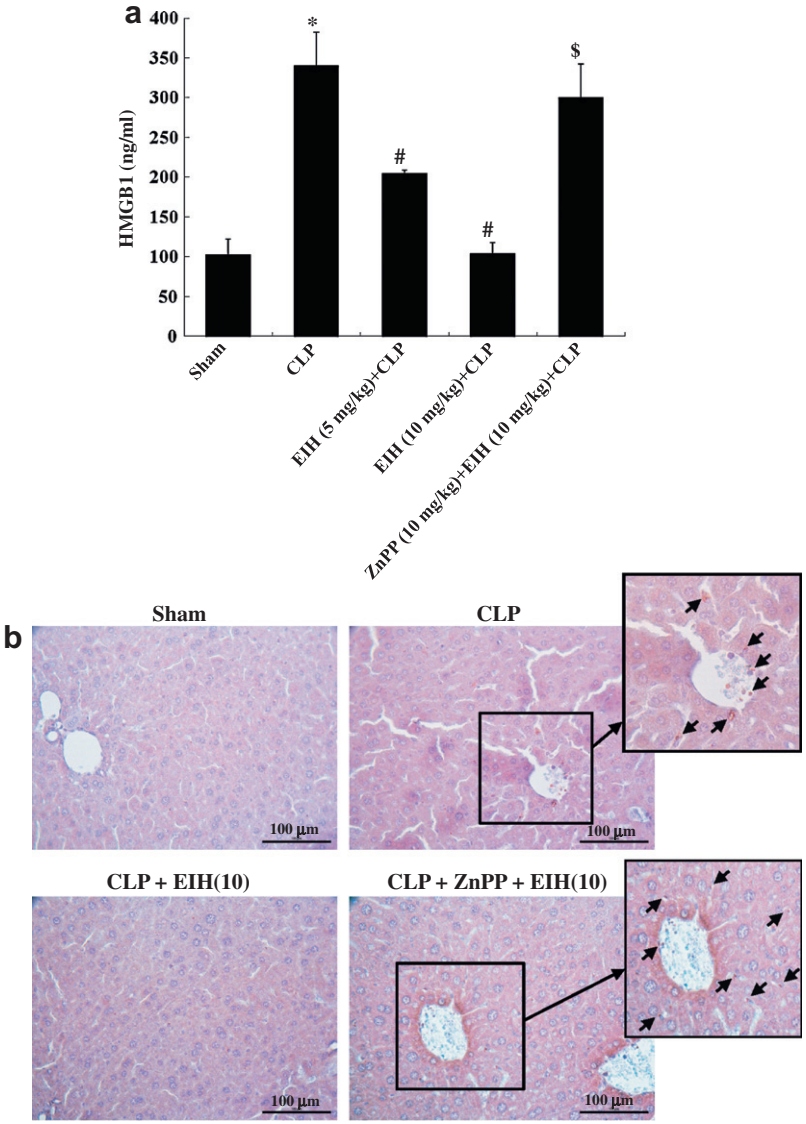

Fig. 8. HO-1-dependent effect of EIH on blood HMGB1 level in CLP-induced septic mice. CLP was performed as described in Section 2. After 24 h of CLP treatment, blood was collected by cardiac puncture from the anesthetized mice. Two different concentrations (5 and 10 mg/kg, i.p.) of EIH or ZnPP IX (10 mg/kg, i.p.) were injected 2 h prior to CLP treatment. HMGB1 level was determined using an ELISA kit (a). EIH reduces inflammatory cell infiltration in the liver tissues of CLP-induced septic mice in a ZnPPIX-sensitive manner. Enlarged insert shows infiltrated F4/80-positive cells in liver tissues (b). The results are expressed as the means ± SE. $^{*}p < 0.05$ compared with Sham animals. $^{\#}p < 0.05$ compared CLP animals. $^{\$}p < 0.05$ compared EIH (10 mg/kg) CLP animals.

activity (Niedick et al., 2004; Reboll et al., 2011). The transcription factor NF-κB is implicated in the regulation of many genes that code for mediators of immune, acute-phase, and inflammatory responses, including iNOS and COX-2. The p50/p65 heterodimer is the most common dimer found in the NF-κB signaling pathway (Verma et al., 1995). Under basal conditions, NF-κB is sequestered in the cytoplasm by inhibitor proteins, usually IκB, whereas upon release, NF-κB dimers translocate to the nucleus to activate target genes by binding with high affinity κB elements in their promoters. Here, we found that EIH dose-dependently inhibited NF-κB activity by demonstrating the dose-dependent inhibition of IκBα phosphorylation and luciferase activity in cells activated with LPS. Therefore, the anti-inflammatory effects of EIH are closely related with inhibition of p65 activation. To further confirm that NF-κB is a target for the anti-inflammatory action of EIH, we investigated the expression of adhesion molecules (ICAM-1 and VCAM-1), which depends on NF-κB activity, in TNF-α-activated endothelial cells (Kim et al., 2006). This finding may be significant in that EIH can provide new therapeutic potential for vascular inflammatory disorders such as atherosclerosis. In this regard, it is interesting to mention that HMGB1 has been reported to be expressed in human atherosclerotic legions (Kalinina et al., 2004). In addition, HO-1 is among those Nrf2-target genes that are significantly expressed in all main cell types present in mouse and human atherosclerotic lesions, such as endothelial cells, macrophages, and smooth muscle cells (Wang et al., 1998; Ishikawa et al., 2001). HO-1 expression in endothelial cells leads to decreased expression of VCAM-1 as well as the expression and release of chemokines and pro-inflammatory cytokines such as CC-chemokine ligand 2, also known as MCP-1 (Sacerdoti et al., 2005). Therefore, further study is needed to determine whether or not EIH would be beneficial to the treatment of atherosclerosis. Previously, we reported that HMGB1 is associated with sepsis-induced lethality in an animal model, and LPS releases HMGB1 in RAW 264.7 cells. In addition, it was found that the HMGB1 level was higher in HO-$1^{-/-}$ mice than HO-$1^{+/+}$ mice when animals were subjected to either LPS injection or CLP-induced

polymicrobial sepsis, indicating that HO-1 inversely regulates HMGB1 under septic conditions (Tosyi et al., 2011a; Takamiya et al., 2009). It is important to provide evidence that the anti-inflammatory effect of EIH *in vivo* is mediated through HO-1. Therefore, we used a CLP-induced septic mice model. It is clear that the anti-inflammatory action of EIH *in vivo* is dependent on HO-1 activity, as its protective effects against organ damage were reversed by an HO-1 inhibitor. Another important finding is that blood HMGB1 levels were significantly reduced by EIH in CLP-induced mice, which were restored by the HO-1 inhibitor ZnPP IX, supporting that HO-1 activity negatively regulates HMGB1 under systemic inflammatory conditions. These *in vitro* and *in vivo* data imply that the ability of EIH to mediate anti-inflammatory effects is based on the up-regulation of HO-1 expression via p38 MAPK/Nrf2 activation. From GC/MS analysis, we found that EIH contained isoalantolactone, β-elemene, valencene, and germacrene A (data not shown). Since we reported that valencene induces HO-1 in RAW 264.7 cells (Tsoyi et al., 2011b), it may have contributed to induction of HO-1 by EIH in the present study. However, we found that EIH contained higher amounts of isoalantolactone than valencene, which means further investigation is needed to determine whether or not isoalantolactone induces HO-1 in immune cells.

In summary, we investigated the anti-inflammatory action of EIH in association with induction of HO-1. The present results show that EIH increased HO-1 induction via p38 MAPK/Nrf2 signaling in RAW 264.7 cells, which is critical for anti-inflammatory action. In addition, NF-κB inhibitory action resulted in decreased inflammation as evidenced by inhibition of LPS-activated iNOS, COX-2, and HMGB1 release in RAW 264.7 cells, as well as adhesion molecules in human endothelial cells. Finally, the protective effect of EIH against organ damage was antagonized by ZnPP IX, an HO-1 inhibitor. Thus, induction of HO-1 expression may be an important mechanism in the anti-inflammatory action of EIH.

Conflict of Interest

The authors declare that there are no conflicts of interest.

References

Andersson, U., Erlandsson-Harris, H., 2004. HMGB1 is a potent trigger of arthritis. J. Int. Med. 255, 344–350.

Ardoin, S.P., Pisetsky, D.S., 2008. The role of cell death in the pathogenesis of autoimmune disease: HMGB1 and microparticles as intercellular mediators of inflammation. Mod. Rheumatol. 18, 319–326.

Bustin, M., 1999. Regulation of DNA-dependent activities by the functional motifs of the high-mobility-group chromosomal proteins. Mol. Cell. Biol. 19, 5237–5246.

Dorn, D.C., Alexenizer, M., Hengstler, J.G., Dorn, A., 2006. Tumor cell specific toxicity of *Inula helenium* extracts. Phytother. Res. 20, 970–980.

Ha, Y.M., Kim, M.Y., Park, M.K., Lee, Y.S., Kim, Y.M., Kim, H.J., Lee, J.H., Chang, K.C., 2012. Higenamine reduces HMGB1 during hypoxia-induced brain injury by induction of heme oxygenase-1 through PI3K/Akt/Nrf-2 signal pathways. Apoptosis 17, 463–474.

Ishikawa, K., Sugawara, D., Wang, X., Suzuki, K., Itabe, H., Maruyama, Y., Lusis, A.J., 2001. Hemeoxygenase-1inhibits atherosclerotic lesion formation in ldl-receptor knockout mice. Circ. Res. 88, 506–512.

Jang, H.J., Kim, Y.M., Tsoyi, K., Park, E.J., Lee, Y.S., Kim, H.J., Joe, Y., Chung, H.T., Chang, K.C., 2012. Ethyl pyruvate induces heme oxygenase-1 through p38 mitogen-activated protein kinase activation by depletion of glutathione in RAW 264.7 cells and improves survival in septic animals. Antioxid. Redox. Signal 17, 878–889.

Joe, Y., Zheng, M., Kim, H.J., Kim, S., Uddin, M.J., Park, C., Ryu, do.G., Kang, S.S., Ryoo, S., Ryter, S.W., Chang, K.C., Chung, H.T., 2012. Salvianolic acid B exerts vasoprotective effects through the modulation of heme oxygenase-1 and arginase activities. J. Pharmacol. Exp. Ther. 341, 850–858.

Jun, M.S., Kim, H.S., Kim, Y.M., Kim, H.J., Park, E.J., Lee, J.H., Lee, K.R., Kim, Y.S., Chang, K.C., 2012. Ethanol extract of *Prunella vulgaris* var. lilacina inhibits HMGB1 release by induction of heme oxygenase-1 in LPS-activated RAW 264.7 cells and CLP induced septic mice. Phytother. Res. 26, 605–612.

Kalinina, N., Agrotis, A., Antropova, Y., DiVitto, G., Kanellakis, P., Kostolias, G., Ilyinskaya, O., Tararak, E., Bobik, A., 2004. Increased expression of the DNA-binding cytokine HMGB1 in human atherosclerotic lesions: role of activated macrophages and cytokines. Arterioscler. Thromb. Vasc. Biol. 24, 2320–2325.

Kang, Y.J., Lee, Y.S., Lee, G.W., Lee, D.H., Ryu, J.C., Yun-Choi, H.S., Chang, K.C., 1999. Inhibition of activation of nuclear factor kappaB is responsible for inhibition of inducible nitric oxide synthase expression by higenamine, an active component of aconite root. J. Pharmacol. Exp. Ther. 291, 314–320.

Kim, H.J., Tsoy, I., Park, J.M., Chung, J.I., Shin, S.C., Chang, K.C., 2006. Anthocyanins from soybean seed coat inhibit the expression of TNF-alpha-induced genes associated with ischemia/reperfusion in endothelial cell by NF-kappaB-dependent pathway and reduce rat myocardial damages incurred by ischemia and reperfusion in vivo. FEBS Lett. 580, 1391–1397.

Kim, J.H., Kyung, C.Y., Lee, K.S., Cho, D.H., Baek, Y.Y., Lee, D.K., Ha, K.S., Choe, J., Won, M.H., Jeoung, D., Lee, H., Kwon, Y.G., Kim, Y.M., 2012. Functional dissection of Nrf2-dependent phase II genes in vascular inflammation and endotoxic injury using Keap1 siRNA. Free Rad. Biol. Med. 53, 629–640.

Kobayashi, H., Takeno, M., Saito, T., Takeda, Y., Kirino, Y., Noyori, K., Hayashi, T., Ueda, A., Ishigatsubo, Y., 2006. Regulatory role of heme oxygenase 1 in inflammation of rheumatoid arthritis. Arth. Rheum. 54, 1132–1142.

Konishi, T., Shimada, Y., Nagao, T., Okabe, H., Konoshima, T., 2002. Antiproliferative sesquiterpene lactones from the roots of *Inula helenium*. Bio. Pharm. Bull. 25, 1370–1372.

Lotze, M.T., Tracey, K.J., 2005. High-mobility group box 1 protein (HMGB1): nuclear weapon in the immune arsenal. Nat. Rev. Immunol. 5, 331–342.

Naidu, S., Vijayan, V., Santoso, S., Kietzmann, T., Immenschuh, S., 2009. Inhibition and genetic deficiency of p38 MAPK up-regulates heme oxygenase-1 gene expression via Nrf2. J. Immunol. 182, 7048–7057.

Niedick, I., Froese, N., Oumard, A., Mueller, P.P., Nourbakhsh, M., Hauser, H., Köster, M., 2004. Nucleolar localization and mobility analysis of the NF-kappaB repressing factor NRF. J. Cell. Sci. 117 (Pt 16), 3447–3458.

Otterbein, L.E., Lee, P.J., Chin, B.Y., Petrache, I., Camhi, S.L., Alam, J., Choi, A.M., 1999. Protective effects of heme oxygenase-1 in acute lung injury. Chest 116 (1 Suppl.), 61S–63S.

Pullikotil, P., Chen, H., Muniyappa, R., Greenberg, C.C., Yang, S., Reiter, C.E., Lee, J.W., Chung, J.H., Quon, M.J., 2011. Epigallocatechin gallate induces expression of heme oxygenase-1 in endothelial cells via p38 MAPK and Nrf-2 that suppresses proinflammatory actions of TNF-α. J. Nutr. Biochem. 23, 1134–1145.

Qiu, J., Luo, M., Wang, J., Dong, J., Li, H., Leng, B., Zhang, Q., Dai, X., Zhang, Y., Niu, X., Deng, X., 2011. Isoalantolactone protects against *Staphylococcus aureus* pneumonia. FEMS Microbiol. Lett. 324, 147–155.

Reboll, M.R., Schweda, A.T., Bartels, M., Franke, R., Frank, R., Nourbakhsh, M., 2011. Mapping of NRF binding motifs of NF-kappaB p65 subunit. J. Biochem. 150, 553–562.

Ryter, S.W., Choi, A.M., 2006. Therapeutic applications of carbon monoxide in lung disease. Curr. Opin. Pharmacol. 6, 257–262.

Sacerdoti, D., Colombrita, C., Ghattas, M.H., Ismaeil, E.F., Scapagnini, G., Bolognesi, M., Volti, G.L., Abraham, N.G., 2005. Heme oxygenase-1 transduction in endothelial cells causes downregulation of monocyte chemoattractant protein-1 and of genes involved in inflammation and growth. Cell. Mol. Biol. 51, 363–370.

Seo, J.Y., Lim, S.S., Kim, J.R., Lim, J.S., Ha, Y.R., Lee, I.A., Kim, E.J., Park, J.H., Kim, J.S., 2008. Nrf2-mediated induction of detoxifying enzymes by alantolactone present in *Inula helenium*. Phytother. Res. 22, 1500–1505.

Shin, J.H., Kim, S.W., Jin, Y., Kim, I.D., Lee, J.K., 2012. Ethyl pyruvate-mediated Nrf2 activation and hemeoxygenase 1 induction in astrocytes confer protective effects via autocrine and paracrine mechanisms. Neurochem. Int. 61, 89–99.

Slot, C., 1965. Plasma creatinine determination. A new and specific Jaffe reaction method. Scand. J. Clin. Lab. Invest. 17, 381–387.

Takamiya, R., Hung, C.C., Hall, S.R., Fukunaga, K., Nagaishi, T., Maeno, T., Owen, C., Macias, A.A., Fredenburgh, L.E., Ishizaka, A., Blumberg, R.S., Baron, R.M., Perrella, M.A., 2009. High-mobility group box 1 contributes to lethality of endotoxemia in heme oxygenase-1-deficient mice. Am. J. Res. Cell. Mol. Biol. 41, 129–135.

Tsoyi, K., Lee, T.Y., Lee, Y.S., Kim, H.J., Seo, H.G., Lee, J.H., Chang, K.C., 2009. Hemeoxygenase-1 induction and carbon monoxide-releasing molecule inhibit lipopolysaccharide (LPS)-induced high-mobility group box 1 release in vitro and improve survival of mice in LPS- and cecal ligation and puncture-induced sepsis model in vivo. Mol. Pharm. 76, 173–182.

Tsoyi, K., Jang, H.J., Nizamutdinova, I.T., Kim, Y.M., Lee, Y.S., Kim, H.J., Seo, H.G., Lee, J.H., Chang, K.C., 2011a. Metformin inhibits HMGB1 release in LPS-treated RAW 264.7 cells and increases survival rate of endotoxaemic mice. Br. J. Pharmacol. 162, 1498–1508.

Tsoyi, K., Jang, H.J., Lee, Y.S., Kim, Y.M., Kim, H.J., Seo, H.G., Lee, J.H., Kwak, J.H., Lee, D.U., Chang, K.C., 2011b. (+)-Nootkatone and (+)-valencene from rhizomes of *Cyperus rotundus* increase survival rates in septic mice due to heme oxygenase-1 induction. J Ethnopharmacol. 137, 1311–1317.

Verma, I.M., Stevenson, J.K., Schwarz, E.M., Antwerp, D.V., Miyamoto, S., 1995. Rel/NFkappaB/I kappaB family: intimate tales of association and dissociation. Genes Dev. 9, 2723–2735.

Wang, L.J., Lee, T.S., Lee, F.Y., Pai, R.C., Chau, L.Y., 1998. Expression of hemeoxygenase-1 inatherosclerotic lesions. Am. J. Path. 152, 711–720.

Zhang, S., Zhong, J., Yang, P., Gong, F., Wang, C.Y., 2009. HMGB1, an innate alarmin, in the pathogenesis of type 1 diabetes. Int. J. Clin. Exp. Path. 3, 24–38.